Stem Cell Research 33 (2018) 83–94

Contents lists available at ScienceDirect

Stem Cell Research

journal homepage: www.elsevier.com/locate/scr

Pluripotent stem cell-derived interneuron progenitors mature and restore memory deficits but do not suppress seizures in the epileptic mouse brain

Nickesha C. Anderson[a,*], Meghan A. Van Zandt[a], Swechhya Shrestha[a], Daniel B. Lawrence[a,b], Jyoti Gupta[a], Christopher Y. Chen[a], Felicia A. Harrsch[a], Trinithas Boyi[a,b], Carolyn E. Dundes[a], Gloster Aaron[a,b], Janice R. Naegele[a,b], Laura Grabel[a]

[a] Dept. of Biology, Wesleyan University, 52 Lawn Avenue, Middletown, CT 06459, USA
[b] Program in Neuroscience and Behavior, Wesleyan University, 52 Lawn Avenue, Middletown, CT 06459, USA

ARTICLE INFO

Keywords:
GABAergic interneuron progenitors
Embryonic stem cells
Electrophysiological analyses
Hippocampal-dependent spatial memory
Temporal lobe epilepsy

ABSTRACT

GABAergic interneuron dysfunction has been implicated in temporal lobe epilepsy (TLE), autism, and schizophrenia. Inhibitory interneuron progenitors transplanted into the hippocampus of rodents with TLE provide varying degrees of seizure suppression. We investigated whether human embryonic stem cell (hESC)-derived interneuron progenitors (hESNPs) could differentiate, correct hippocampal-dependent spatial memory deficits, and suppress seizures in a pilocarpine-induced TLE mouse model. We found that transplanted ventralized hESNPs differentiated into mature GABAergic interneurons and became electrophysiologically active with mature firing patterns. Some mice developed hESNP-derived tumor-like NSC clusters. Mice with transplants showed significant improvement in the Morris water maze test, but transplants did not suppress seizures. The limited effects of the human GABAergic interneuron progenitor grafts may be due to cell type heterogeneity within the transplants.

1. Introduction

Temporal lobe epilepsy (TLE) is characterized by mild to severe convulsive seizures, aberrant neurogenesis, mossy fiber sprouting, sclerosis and interneuron dysfunction (Parent and Murphy, 2013) and affects approximately 3.4 million individuals in the United States. TLE patients experience seizures that originate in the mesial temporal lobe, primarily affecting hippocampal function. The direct causes of TLE are not fully understood; however traumatic brain injury, stroke, tumors and focal lesions have been associated with the disease (Cascino et al., 1992; Wolf et al., 1993). Interneuron loss and inhibitory neural circuit dysfunction are thought to be key to epileptogenesis and development of temporal lobe seizures (de Lanerolle et al., 1989; de Lanerolle et al., 2010, 2012). TLE patients and animal models commonly exhibit behavioral and cognitive changes, including learning and memory deficits (Hermann et al., 2002; Jokeit and Ebner, 1999). While antiepileptic drugs can be effective at suppressing seizures in a subset of patients, they do little to repair dysfunctional neural circuitry, and approximately one third of patients are refractory to drug-based therapies. For many patients, surgical removal of the hippocampus is the only option. The lack of effective treatment options led to attempts to develop effective cell replacement therapies using GABAergic interneuron progenitors (Parent and Murphy, 2013).

There are two potential sources of interneuron progenitors: fetal material or pluripotent stem cells (PSCs). Cells can be isolated from the embryonic ventral forebrain region known as the medial ganglionic eminence (MGE), the major source of parvalbumin (PV)- and somatostatin (SST)-expressing interneurons affected in TLE (Anderson et al., 2001; Kepecs and Fishell, 2014; Shetty and Hattiangady, 2007). During embryonic development, MGE-derived interneuron progenitors are generated in an environment of high sonic hedgehog (SHH) concentration, characterized by the expression of the transcription factor NKX2.1 (Sussel et al., 1999). Knockout of SHH signaling in E12.5 mice results in failure to initiate and maintain expression of NKX2.1, leading to a deficiency in PV and SST cortical interneurons (Machold et al., 2003; Xu et al., 2005). Some interneuron progenitors are also generated in the caudal ganglionic eminence (CGE), the lateral ganglionic eminence (LGE), and the preoptic area (PoA) (Flames et al., 2007; Gelman

* Corresponding author at: Shanklin Hall Atwater Labs, Biology Department, 52 Lawn Ave, Middletown, CT 06459, USA.
E-mail addresses: ncanderson@wesleyan.edu (N.C. Anderson), mvanzandt@wesleyan.edu (M.A. Van Zandt), sshrestha@wesleyan.edu (S. Shrestha), dblawrence@wesleyan.edu (D.B. Lawrence), jgupta@wesleyan.edu (J. Gupta), cychen@wesleyan.edu (C.Y. Chen), tboyi@wesleyan.edu (T. Boyi), cdundes@stanford.edu (C.E. Dundes), gaaron@wesleyan.edu (G. Aaron), jnaegele@wesleyan.edu (J.R. Naegele), lgrabel@wesleyan.edu (L. Grabel).

https://doi.org/10.1016/j.scr.2018.10.007
Received 10 March 2018; Received in revised form 27 August 2018; Accepted 3 October 2018
Available online 05 October 2018

and Marin, 2010; Hansen et al., 2013; Ma et al., 2013).

Fetal MGE-derived GABAergic progenitors grafted to the hippocampus of adult epileptic rodent models can differentiate, suppress seizures, and correct spatial memory deficits (Baraban et al., 2009; Hammad et al., 2015; Henderson et al., 2014; Hunt et al., 2013; Loscher et al., 1998; Waldau et al., 2010; Zipancic et al., 2010), highlighting the potential of embryo-derived GABAergic interneuron progenitors for the treatment of TLE. However, the use of human fetal material would be costly, fraught with ethical concerns, and challenging to standardize. We, and others, have therefore focused on generating GABAergic interneuron progenitors from a PSC source (Cunningham et al., 2014; Germain et al., 2013; Kim et al., 2014; Maroof et al., 2013; Nicholas et al., 2013).

Identification of the conditions that specify interneuron progenitors during early embryonic development has directed the design of protocols that promote differentiation of PSCs into interneuron progenitors *in vitro*. These approaches typically involve treatment with SHH and the Smoothened agonist purmorphamine (Pur) to ventralize the neural stem cell (NSC) population. Combinatorial BMP and TGF-β inhibition, followed by SHH treatment, promotes production of MGE-like interneuron progenitors while inhibiting dorsal and CGE-like cell types (Li et al., 2009). An appropriate SHH treatment window, duration, and concentration is essential for generating specific interneuron progenitor subtypes *in vitro* (Germain et al., 2013; Goulburn et al., 2012; Kim et al., 2014; Maroof et al., 2013; Nicholas et al., 2013; Tyson et al., 2015). Numerous studies have shown that both embryonic stem cell (ESC) and induced pluripotent stem cell (iPSC)-derived interneuron progenitors can differentiate into interneurons and display mature electrophysiological properties both *in vitro* and *in vivo* (Chen et al., 2016; Germain et al., 2013; Goulburn et al., 2012; Kim et al., 2014; Liu et al., 2013a; Liu et al., 2013b; Maroof et al., 2013; Nicholas et al., 2013).

To test the efficacy of PSC-derived interneuron therapies, *in vitro*-derived interneuron progenitors have been transplanted into rodent models of schizophrenia, Alzheimer's disease, bladder dysfunction and neuropathic pain from spinal cord injury, and TLE (Chohan and Moore, 2016; Cunningham et al., 2014; Etlin et al., 2016; Fandel et al., 2016; Shetty and Bates, 2016). In a study designed to test whether human ESC-derived GABAergic interneuron progenitors would integrate into the hippocampus of pilocarpine-induced TLE mice, ESC-derived GABAergic progenitors transplanted to the hippocampus suppressed seizures over a brief time period (Cunningham et al., 2014). Suppression was attributed to transplant-derived inhibitory currents onto endogenous hippocampal neurons.

We previously reported a monolayer culture system for differentiation of MGE-like interneuron progenitors from hESCs (Germain et al., 2013) and substantiated this cell type identity using transcriptome profiling and *in vitro* long-term differentiation into interneuron subtypes (Chen et al., 2016). Here, we investigated the ability of hESNPs to mature, correct behavioral deficits, and suppress seizures in status epilepticus (SE) mice. We show that hESNPs grafted into the hippocampus of SE mice differentiate into mature inhibitory interneuron subtypes. A subset of animals that received hESNP transplants developed tumor-like clusters that contained some NSCs, but were comprised primarily of mature neurons. Grafted cells exhibited five different types of firing patterns including highly adapting, fast-spiking, bursting, accommodating, and non-accommodating patterns. Cells also showed inhibitory post-synaptic currents (IPSCs) as well as excitatory post-synaptic currents (EPSCs). We observed significant improvement in the spatial memory of SE mice that received transplants. EEG analyses conducted continuously for a 4-week period, showed no statistically significant effect on seizure suppression. These effects were not due to tumor-like NSC clusters or failure of the human interneuron progenitors to engraft and migrate in the host brains, because significant numbers of ESNPs differentiated into neurons that displayed mature electrophysiological properties.

2. Experimental procedures

2.1. Neural induction and differentiation

Neural differentiation and long-term astrocyte-hESNP co-culture were conducted as described (Chen et al., 2016). Differentiating cells were treated with LDN, SHH and Pur. After 18 days, differentiating colonies were plated onto polyL/laminin-coated substrates for further characterization, for long-term co-culture, or frozen in liquid nitrogen for subsequent transplantation.

2.2. Neural progenitor transplantation

All experiments involving the use of animals were performed in accordance with the approved Wesleyan University Animal Care and Use Committee protocols and in accordance with the National Institute of Health Guide for the Care and Use of Laboratory Animals.

Mice used for transplantation were anesthetized using isoflurane gas and carefully monitored throughout the duration of the procedure. After 22–30 days in culture, hESNPs were stereotactically injected bilaterally into the hippocampus of adult NSG mice using a Quintessential injector at the following coordinates: (A/P-2.4, M/L-2.2, D/V-2.2, 2.0). 100,000 cells suspended in 1 μL of media were injected into each hippocampus over a 5-min period.

2.3. Pilocarpine and drug administration

At the time of seizure induction, male and female mice were 6 weeks of age and 18-22 g body weight and maintained on a 12-h light/dark cycle with constant temperature, food and water. Seizures were induced as described previously using a dose of 280 mg/kg (Henderson et al., 2014). One hour following the onset of SE, midazolam was injected to attenuate SE. Ringer's solution was administered, and the mice were returned to individual cages and monitored daily. Two weeks after SE induction, each mouse underwent two weeks of continuous video monitoring using a LOREX system to verify the occurrence of spontaneous recurrent seizures (SRS).

2.4. Electrode implantation and Video-Electroencephalography (V-EEG)

Surgical implantation of subdural electrodes and V-EEG was performed as described previously, with slight modifications (Henderson et al., 2014). Continuous V-EEG recordings were conducted approximately 3 months after transplantation for 30 days. Synchronized video-EEG recordings were captured using either Stellate Harmonie V-EEG system or Pinnacle Technology EEG systems. EEGs were time-synchronized with continuous Mpeg4 video recordings. We employed software algorithms for seizure detection (see supplemental experimental procedures). Ictal events were identified from the V-EEG recordings as generalized discharges of high-frequency, high-voltage polyspikes lasting longer than 10 s. Each seizure was manually verified by trained observers from the corresponding video recordings.

2.5. Behavior analysis - Morris water maze

Spatial memory encoding and recall in SE-induced control and hESNP-transplant NSG mice were assessed using the Morris water maze. The tank was virtually divided into 4 quadrants and the designated platform area through the tracking program ANY-maze, which monitored mouse behavior through a ceiling-mounted camera above the tank during training and testing. Training was divided into 5 consecutive days, starting with two days of cued learning in which the platform was marked with a red striped flagpole followed by three days of uncued learning with an unmarked platform. Twenty-four hours after the last training trial, mice were given 2 probe trial sessions, lasting 60 s each. During the probe trial, the platform was removed from the water

maze and each mouse was lowered into the center of the water maze and allowed to swim for the full 60 s before being rescued, dried, and returned to the appropriate home cage.

2.6. Cell and tissue collection

Embryonic stem cell derived neural progenitors were fixed with 3.7% formaldehyde in phosphate buffered saline (PBS) for 10 min. For tissue collection, mice were given a lethal dose of pentobarbital (100 mg/kg) and transcardially perfused using 4% paraformaldehyde; the brain was then dissected and post fixed overnight, embedded and cryosectioned at a thickness of 12 μm.

2.7. Immunocytochemistry/Immunohistochemistry

For immunocytochemistry, permeabilization was performed with 0.5% PBS-Triton X-100. Blocking was conducted using 5% Serum in 0.1% PBS-Triton X-100 with 2% bovine serum albumin for 1 h at room temperature. Cells were incubated with primary antibodies overnight at 4 °C, washed, and incubated with secondary antibody at room temperature for 1 h. Nuclear counterstain was performed using Hoechst 33342. See supplemental procedures for details and modifications and a list of antibodies used in this study.

2.8. Imaging and quantification

For cell counts, 4–6 random fields were imaged, total nuclei were counted for each field, and the number and percent of nuclei expressing markers of interest were counted. HuNu- or mCherry/RFP-positive cells in each brain section were counted to identify transplanted human cells. Biocytin filled cells were processed and reconstructed using Adobe Photoshop.

2.9. Electrophysiological analysis and optical methods

Slice preparation and electrophysiology were conducted in accordance with Henderson-Gupta et al., 2014; also see supplemental procedures. Briefly, hESNPs were identified using GFP and/or mCherry expression. Whole-cell current clamp recordings were performed under IR-DIC using pipettes filled with intracellular solution. Voltage changes were measured in response to graded positive and negative current injections of 500 ms duration. Whole-cell voltage clamp recordings were performed under IR-DIC using pipettes filled with intracellular solution at + 10 mV or -70 mV to measure spontaneous IPSCs or EPSCs, respectively. Spontaneous postsynaptic currents were blocked with subsequent application of CNQX. Analog signals were digitized at the sampling rate of 40 kHz using an Intrutech ITC-18 and captured with IGOR software.

2.10. Data and statistical analyses

2.10.1. EEG analysis

The average frequency, duration, and severity of seizures were compared between SE mice with hESNP transplants *vs.* control SE mice that had injections of cell culture media into the hippocampus. Seizure data from the entire recording interval for each mouse were included in the analyses. A negative binomial model, which takes into account the differences in the duration of V-EEG recording interval in each mouse, was used to test for differences in seizure frequency between the groups. A two-tailed student *t*-test was used to compare the average duration of seizures. A mixed model was used to compare seizure severity between treatment groups.

2.10.2. Behavior

Analysis was performed using ANY-maze to determine swim speed, swim path length, time spent in each quadrant, escape latency, latency to first platform crossing during probe, and number of platform area entries during probe trials. Data were further analyzed in SPSS for statistics. The two-way repeated measures ANOVA was used to compare latency over time during training between experimental groups while a student *t*-test was used to compare single day probe trial performance values between naïve mice, media injected controls and transplant mice. Mice with confirmed hESNP-derived neural tumor-like NSC clusters were excluded from behavioral data analysis.

2.10.3. Electrophysiology

Current clamp recordings were analyzed with IGOR software to measure the AP rate, half-width, adaptation, repolarization speed and Rin. An ANOVA with Tukey's multiple comparison test was utilized to compare electrophysiological characteristics.

3. Results

3.1. hESNPs mature into interneuron subtypes in vitro

hESNPs generated using a previously described protocol were 98% nestin and 92% Musashi-1 (Msi1) positive NSCs between day 18 and 21 of differentiation (Fig. 1A, B) (Chen et al., 2016; Germain et al., 2013). Based upon immunocytochemical analysis, 55% of the NSCs expressed the interneuron progenitor marker NKX2.1:GFP, and about 9% expressed the neuronal marker MAP2 at day 18 of differentiation (Fig. 1A, C), indicating that at this early time point, the ventralized population primarily consisted of immature NSCs. After 14 weeks in co-culture with mouse astrocytes, 70% of the surviving cells were derived from the hESCs, based upon expression of human nuclear antigen (HuNu), but this decreased to 50% after 17 weeks, indicating decline in survival of human cells (Fig. 1D, E). 30% of HuNu positive cells continued to express the interneuron progenitor marker NKX2.1:GFP at 14 and 17 weeks of differentiation (Fig. 1D, F). Down-regulation of NKX2.1:GFP expression from 55% at day 18 to 30% at 14 and 17 weeks is consistent with the pattern observed upon maturation of cortical interneurons in the mouse embryonic brain (Fig. 1A, D). As the percentage of cells positive for NKX2.1:GFP decreased, the percentage of HuNu expressing cells that co-expressed MAP2 increased to 81.3% (Fig. 1A, D, G), confirming maturation of hESNPs over time. Of the mature HuNu/MAP2 double-positive cell population, 82.5% and 73.1% expressed the neurotransmitter GABA, respectively, at 14 and 17 weeks (Fig. 1D, H), suggesting most of the hESC-derived neurons are inhibitory. Additionally, after 14 and 17 weeks *in vitro*, 30–45% of HuNu/MAP2 double-positive cells expressed the interneuron subtype marker calbindin (CB), while SST expression increased from 5.8% to 14.8% (Fig. 1D, J). We also observed expression of calretinin (CR)/NKX2.1:GFP double-positive 'MGE-like' hESC-derived neurons as well as CR-positive/NKX2.1: GFP negative 'CGE-like' interneurons after 17 weeks in culture (Fig. 1K-K′). Our differentiation protocol yields 55–60% NKX2.1 positive interneuron progenitors, expected to produce MGE-like interneurons, while the remaining 40–45% of the population that is NKX2.1 negative could generate the CGE-like interneuron population observed. We assayed for PV positive cells but did not detect any at 14 and 17 weeks; however, < 1% of hESC-derived neurons expressed PV after 20 weeks (data not shown).

To further examine neuronal maturation, we investigated expression of synaptic proteins using immunocytochemistry. At 17 weeks *in vitro,* we detected expression of synapsin and synaptic vesicle 2 protein (SV2) along the soma and dendrites of hESC-derived NKX2.1:GFP positive neurons co-cultured with mouse cortical astrocytes (Fig. 1L- M′). Using patch clamp analysis, we tested the ability of the hESC-derived neurons to fire action potentials (APs) at 10–20 weeks of culture (Fig. 1N). Ten of the 23 cells patched did not evoke APs in response to current injection (data not shown). Following 50pA current injection over 500 ms duration, patched cells fired a single AP at 10 weeks of differentiation (Fig. 1O) and a burst of APs that display an

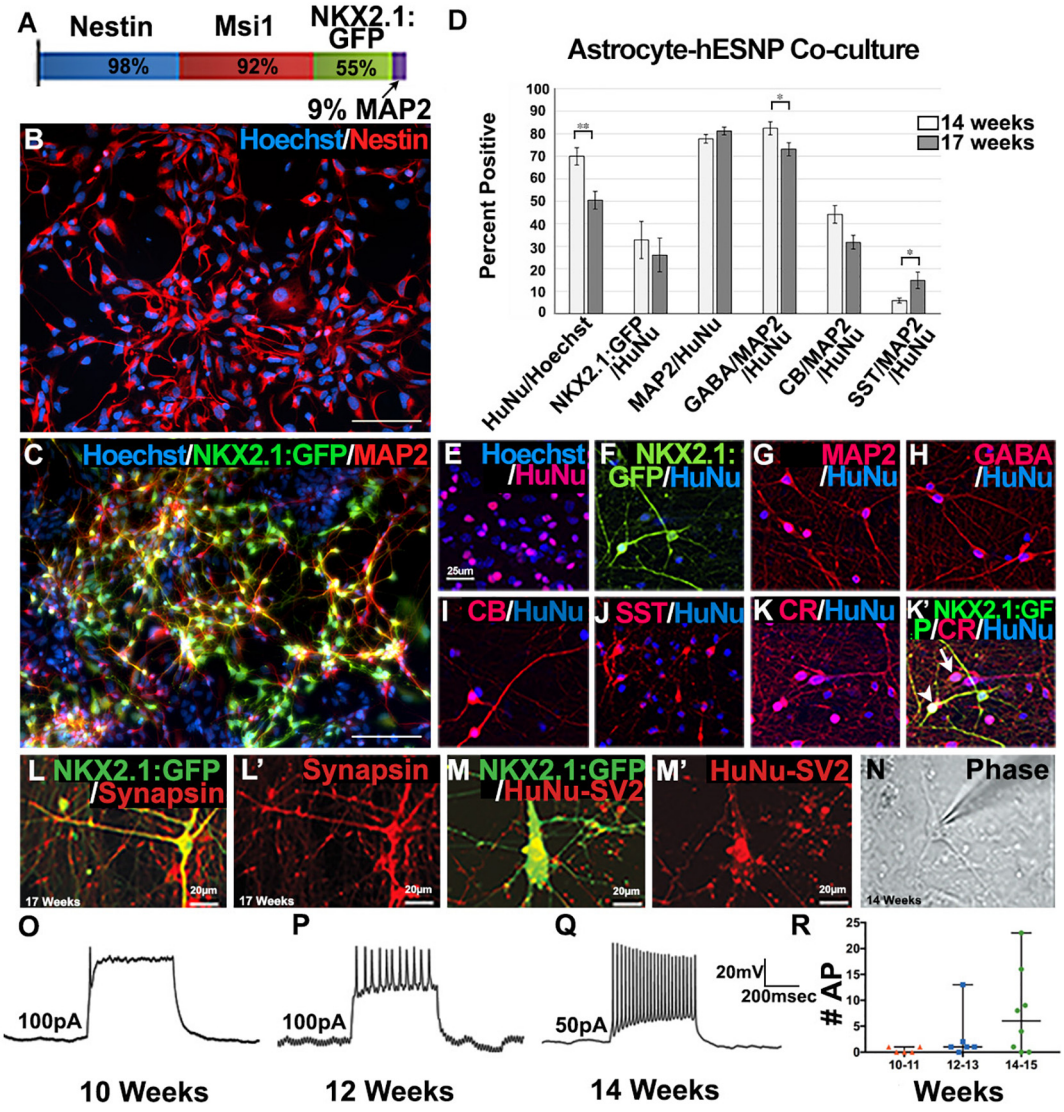

Fig. 1. hESNPs mature into interneuron subtypes *in vitro*.
A) Immunocytochemistry-based quantification of differentiation day (DD) 21 hESNPs. B-C) Representative photomicrograph of hESNPs at DD 30 *in vitro*, scale bars = 100 μm. D) Immunocytochemistry-based quantification of hESC-derived neurons co-cultured with mouse cortical astrocytes, error bars SD, ** = $p < .005$, * = $p < .05$. *E- M′*) Representative photomicrographs of co-cultured neurons at 17 weeks of differentiation, scale bars E-K = 25 μm, L = M′ = 20 μm. MGE-like NKX2.1: GFP/CR-double-positive cells (K′, white arrowheads) and CGE-like NKX2.1: GFP-negative/CR-positive (K′, white arrow). N) DIC image of hESC-derived cell undergoing patch clamp recording. O-Q) Representative electrophysiological recordings from hESC-derived neurons following current injection over 500 ms duration. R) Scatter plot showing increasing number of action potentials evoked in response to current injection over time.

accommodating phenotype at 12 and 14 weeks of differentiation (Fig. 1P-Q). Though not statistically significant, the number of APs evoked in response to current injection gradually increased between 10 and 15 weeks (Fig. 1R), consistent with increasing electrophysiological maturity over time. The inability of some cells to fire a train of APs at 14 weeks of differentiation indicates heterogeneity of the hESC-derived cell population. Overall, these data indicate that hESNPs are able to differentiate into mature neurons expressing synaptic proteins and capable of firing APs.

3.2. hESNPs differentiate into mature GABAergic interneurons after transplantation

To assess hESNP survival, cells were initially transplanted into the DG of naïve mice (Fig. S1). At the time of transplantation, 98% and 92% of the cells were nestin and Musashi-positive respectively and 55% of the neural progenitors expressed NKX2.1:GFP (Fig. 1A). Following initial transplantation, hESNP survival rates, calculated as percent of injected cells (in mice that did not display tumor-like clusters), were 60.6% ± 8.3% ($n = 3$) at 16 weeks post-transplantation. At 15 weeks after transplantation, NKX2.1:GFP/Ubi:RFP positive cells were located throughout the hilus of the DG (Fig. S2A−C) and on either side of the granule cell layer (Fig. S2D−H). Overall, transplantation of hESNPs into naïve mice indicated good survival, differentiation, and dispersal of cells throughout the DG. Additional transplantation experiments were performed in mice with pilocarpine-induced SE. Seizure activity, electrophysiology and immunohistochemical analyses were conducted at various time points 6 to 24 weeks post-transplantation (Fig. 2A). Reconstructions of bilaterally transplanted RFP-positive hESNPs in the hippocampus of SE mice at 6 weeks (Fig. S2I) verified survival of transplanted cells in the DG. Grafted cells were primarily located in the dorsal (Fig. S2J) to medial (Fig. S2K) half of the hippocampus after 16.5 weeks *in vivo*. HuNu-expressing cells, positive for NKX2.1:GFP, were located in the DG of the hippocampus (Fig. 2B). Expression of nestin (Fig. 2C, O) and DCX (Fig. 2D, O) confirmed that 6 weeks after transplantation, 37% of transplanted RFP-positive cells remained as

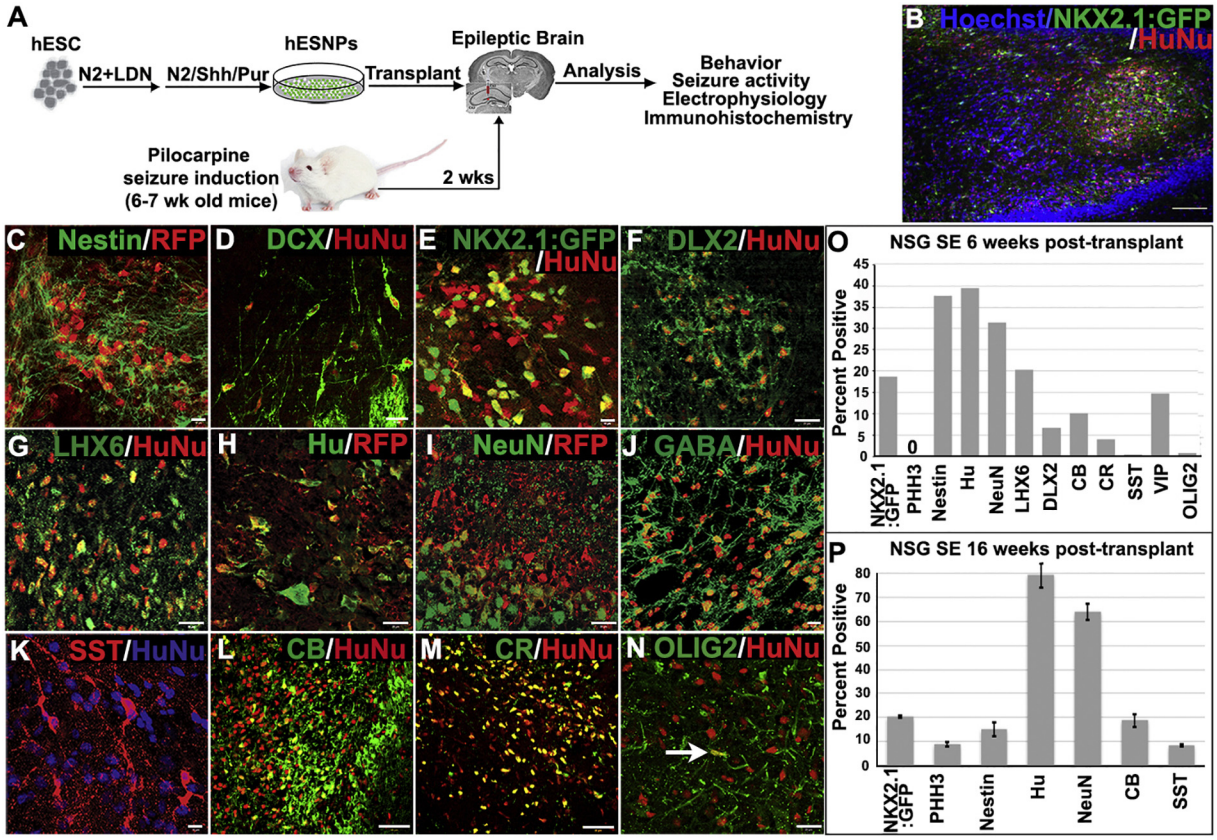

Fig. 2. hESNPs differentiate into mature GABAergic interneurons after transplantation into SE mice. See also Figs. S1 and S2.
A) Transplant scheme. B-N) Representative immunohistochemistry photomicrographs of transplanted hESNPs at 16 weeks, scale bars, B = 100 μm, C-*N* = 20 μm. O-P) Immunohistochemistry-based quantification at 6 (n = 1) and 16 weeks (n = 3) post-transplantation. Error bars show S.E.M.

NSCs. Continued expression of NKX2.1:GFP (Fig. 2E), DLX2 (Fig. 2F), and LHX6 (Fig. 2G) 6 weeks after transplantation confirmed inhibitory progenitor cell identity.

Despite persistence of an interneuron progenitor population, 30–40% of transplanted cells became mature Hu- (Fig. 2H, O; S1D″) and NeuN- (Fig. 2I, O; S1D‴) positive neurons by 6 weeks. Over time, transplanted hESNPs continued to differentiate, as the percentage of Hu and NeuN expressing cells increased from 40% and 31% at 6 weeks (Fig. 2O), to 80% and 65%, respectively, by 16 weeks. As the cells matured, they began to produce GABA (Fig. 2J), verifying the inhibitory identity of some of the differentiated interneurons. Furthermore, we identified SST (Fig. 2K, O; S1E″), CB (Fig. 2L, O; S1E′) and CR (Fig. 2M, O) interneuron subtypes as early as 6 weeks post-transplantation. SST positive cells increased from < 1% at 6 weeks (Fig. 2O), to over 10% at 16 weeks (Fig. 2P). Similarly, the percent of CB expressing cells doubled from 10% at 6 weeks (Fig. 2O) to 20% at 16 weeks (Fig. 2P). While PV expression was not detected at 6 or 16 weeks, small clusters of cells expressing PV were present 22 weeks after transplantation into naïve mice (Fig. S3F). We assayed for the oligodendrocyte marker OLIG2, and found < 1% OLIG2 positive cells (Fig. 2N, O) after 6 weeks, consistent with the absence of glial derivatives. Overall, following transplantation of hESNPs to the hippocampus, we saw a similar profile of differentiation as observed with *in vitro* long-term cultures. For example, SST-, CB-, and CR-expressing interneurons emerged after 12 weeks of differentiation both *in vitro* and *in vivo*.

3.3. hESC-derived tumor-like NSC clusters in some naive and SE mice are composed of mixtures of NSCs and mature interneurons

The major disadvantages of transplanting neural progenitors from a pluripotent source are possible teratocarcinoma formation from undifferentiated cells and tumor formation from immature cells. We observed that batches of transplanted cells produced tumor-like NSC clusters in naive (29%) and SE animals (18%). The main distinguishing feature utilized to characterize tumors was the presence of rosette-like proliferative NSC clusters. In addition, some cell overgrowths caused disruption of brain structures and transplanted cells were not well integrated. In some animals that received bilateral transplants (Fig. 3A-B), we observed NSC cluster formation in only one hemisphere (Fig. 3B). Some NSC clusters exhibited well-defined borders (Fig. 3B), while others appeared more dispersed throughout the hippocampus and surrounding brain regions (Fig. S3A).

Importantly, all HuNu-positive cells within the NSC clusters were negative for the expression of the pluripotency marker OCT4, the endoderm marker Troma1, and the mesodermal cell marker smooth muscle actin (SMA) (Fig. 3C-E), indicating that they were not teratocarcinomas. To further characterize the tumor-like NSC clusters, we tested whether they contained proliferative cells as late as 12–24 weeks after transplantation and found that between 4 and 10% of the cells were Ki67-positive (Fig. 3F), indicating that there was a persistent population of dividing cells. Moreover, approximately 30% of cells within clusters were NSCs, identified by nestin expression (Fig. 3H), and these cells could self-organize into neural rosette-like structures (Fig. 3H, dotted white line), with a surrounding zone of more mature cells, reminiscent of proliferative zones observed in cerebral organoids (Lancaster et al., 2013).

Although proliferative nestin-positive cells were identified in some mice, a majority of the HuNu-positive cells in transplants with tumor-like NSC clusters expressed neuronal markers characteristic of differentiating human neurons including, DCX, β-III tubulin, Hu, and NeuN (Fig. 3I-L, Fig. S3 B-D) and interneuron markers NKX2.1: GFP, DLX2, LHX6, CB, CR, and SST (Fig. 3M-Q, S3). The hippocampus containing

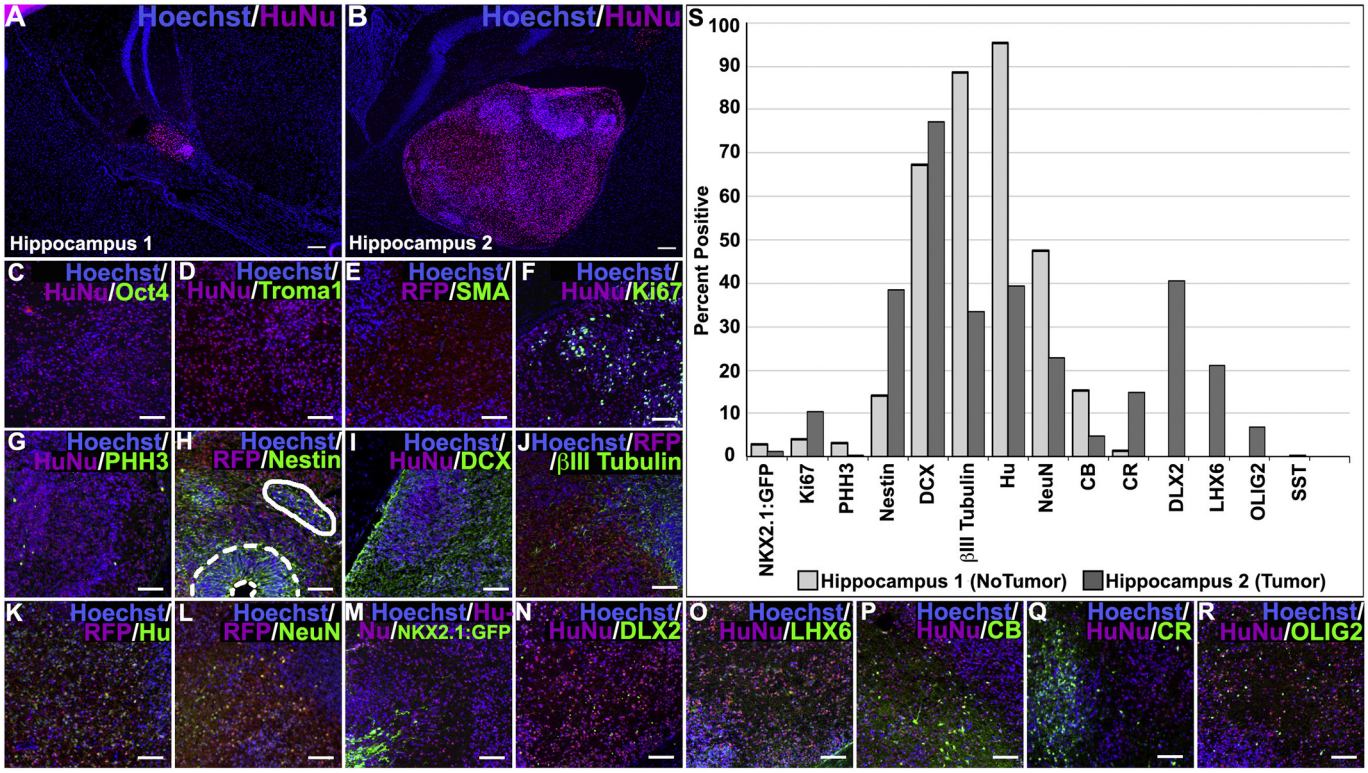

Fig. 3. hESC-derived tumor-like NSC clusters in some naive and SE mice are composed of mixtures of NSCs and mature interneurons. See also Fig. S3.
A-B) Photomicrograph of HuNu positive cells (red) in each hemisphere of a single mouse brain 12 weeks after transplantation, scale bars = 100 μm. C-R) Representative photomicrographs of transplanted HuNu-positive hESC-derived cells. Dotted and solid white lines in panel H highlight nestin positive NSC clusters, scale bars = 50 μm. S) Immunohistochemistry-based quantification of transplanted cells with and without tumor-like NSC clusters. Note: Due to the small size of the transplant in hippocampus 1, we were unable to ascertain percentages of DLX2, LHX6, OLIG2 and SST.

tumor-like NSC clusters generally contained a higher proportion of NSCs and DCX-positive migratory neuroblasts, while the hippocampus with no visible NSC clusters had a greater percentage of mature neurons. After longer periods following transplantation, discrete clusters of neurons (Fig. S3A, white box), emerged within the transplants, containing interneuron subsets that expressed DLX2, PV, and CB (Fig. S3 B-G), but no VIP, CR, LHX6, OLIG2, or SST (Fig. S3 H-L). In other domains, clustered expression was found for different subtypes of MGE-like forebrain interneurons expressing CR, SST, and DLX2 (Fig. S3 M-O). These findings suggest that the proliferating NSCs give rise to clusters of functionally related cells within the transplant. Overall, our data indicate that hESC-derived hESNPs maintain a population of dividing NSCs that have the potential to generate tumor-like NSC clusters after transplantation into the brain.

3.4. Transplanted hESNPs differentiate into mature electrophysiologically active neurons

To investigate the maturation and synaptic activity of hESNPs, we performed whole-cell patch clamp recordings of transplanted cells in hippocampal slices. We patched a total of 126 transplanted cells, of these, 86 biocytin-filled cells were recovered for morphological imaging. Fourteen of the recorded neurons were from transplants in epileptic mice, 112 were from transplants in naïve mice and 100 were localized in tumor-like clusters. Cells that evoked fewer than three APs were excluded from further analyses. Based upon varying firing patterns, the cells were divided into five categories, Types I−V (Fig. 4A, S4-S5). Type I cells (17.3%) displayed highly adapting firing patterns, Type II cells (3.7%) resembled fast-spiking interneurons, Type III cells (11.1%) exhibited initial burst firing, Type IV cells (29.5%) displayed strong accommodating firing patterns and Type V cells (37.3%) displayed little to no accommodating firing patterns. Type III, IV, and V were further subdivided into two groups, with and without after-hyperpolarization (AHP). The larger AHP among different cells within groups III-V is suggestive of a greater number of K_{Ca} channels. Type I cells had significantly lower AP rates than Types II-V, and also displayed higher half-widths, higher adaptations, and slower repolarization speeds, indicating a more immature cell population (Fig. 4B, Table 1). Type II cells exhibited high AP rates, small AP half-widths, fast AHP, low adaptations, high repolarization speeds, and low input resistance, consistent with the characteristics of endogenous fast-spiking cells (Fig. 4B, Table 1). When compared to Type I cells, Types IV and V cells displayed significantly higher AP rates, suggesting that these groups were composed of more mature transplanted cells (Fig. 4B, Table 1). Notably, Type IV consisted of two cells (indicated by the asterisk, Fig. S4) that displayed some degree of negative adaptation. Overall, as the AP rate increased between the cell types, there was a decrease in adaptation, and an increase in repolarization speed, allowing for a greater number of APs to be evoked over the stimulus duration.

Voltage clamp recordings at -70 mV and + 10 mV revealed both EPSCs and IPSCs in hESNPs (Fig. 4C). The average time constant (τ) for EPSCs was 4.48 ± 0.91 ms and for IPSCs was 27.8 ± 2.1 ms, calculated with single exponential curve fitting. Likewise, EPSCs recorded at -70 mV were abolished with the application of 10 μM CNQX (AMPA receptor antagonist) (Fig. 4D), indicating that hESNPs were receiving excitatory synaptic inputs.

3.5. SE mice with hESNP transplants show significant improvements in cognition at 6 and 10 weeks post-transplantation

Pilocarpine-induced SE in rodents results in significant impairments in tests of spatial memory (Muller et al., 2009). Moreover, studies have reported that mouse or human interneuron grafts can ameliorate

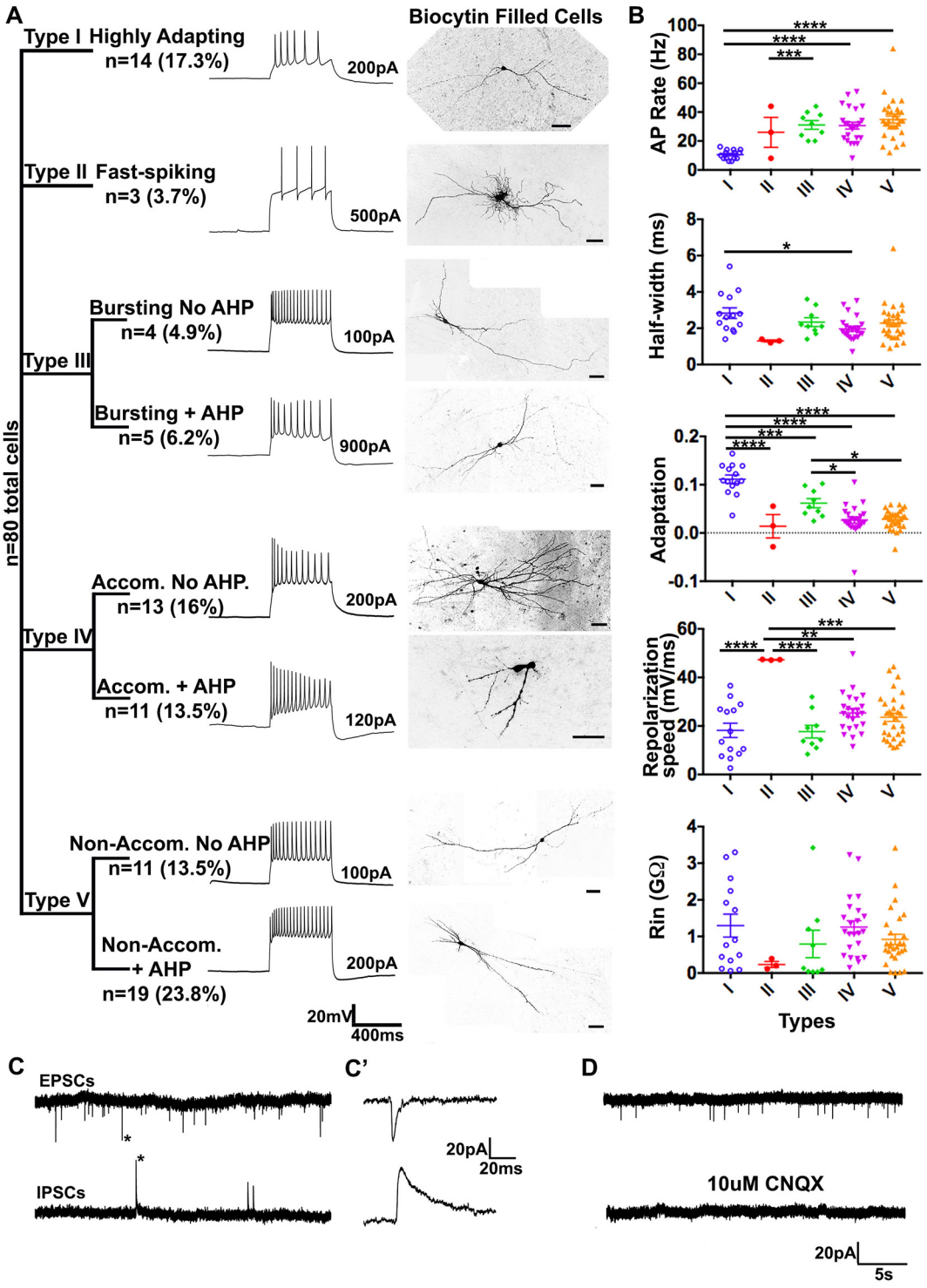

Fig. 4. Transplanted hESNPs differentiate into mature electrophysiologically active neurons. See also Figs. S4 and S5.
A) The analyzed electrophysiological recordings (n = 80) were subdivided into five categories based on their firing patterns. Type 1 (n = 14), Type II (n = 3), Type III (n = 9), Type IV (n = 24), Type V (n = 30). Representative firing patterns of each type (left) and their corresponding morphologies (right). Type III, IV and V were further subdivided into two groups, scale bars = 50 μm. B) Graphs showing AP rate, AP half-width, adaptation, repolarization speed, and input resistance (Rin) of the five different firing types. Results are represented as mean ± SEM (ANOVA with Tukey's multiple comparison test, **** $p < .0001$, *** $p < .001$, **$P < .01$, *$P < .05$). C) Voltage clamp recordings of transplanted hESNPs at -70 mV and + 10 mV show EPSCs and IPSCs, respectively. (C') Enlarged views of individual EPSCs and IPSCs indicated by asterisk. D) EPSCs recorded at -70 mV were abolished with the application of 10 μM CNQX. AHP = After hyperpolarization.

aspects of memory impairment and other comorbid behavioral impairments associated with TLE, such as increased aggression (Cunningham et al., 2014; Maisano et al., 2012). To examine whether our SE mice with hESNP hippocampal transplants showed cognitive improvements in spatial memory, we tested naïve controls, SE mice with media injections, and SE mice with transplants on the Morris water maze, a hippocampal-dependent spatial memory test. During the 5 day training period, SE mice with transplanted cells showed significantly shorter latencies when compared to media controls (two-way Repeated Measures ANOVA, $p < .05$; Fig. 5A). During the probe trials conducted

Table 1
Electrophysiological properties of transplanted cells with five different types of firing patterns.

AP characteristics	Type I (n = 14)	Type II (n = 3)	Type III (n = 9)	Type IV (n = 24)	Type V (n = 30)	P < .05
AP rate (Hz)	10.57 ± 0.88	26 ± 10.39	31.11 ± 2.98	30.67 ± 2.38	34.9 ± 2.42	I-IV, I–V, II-III
Half-width (ms)	2.83 ± 0.29	1.3 ± 0.58	2.33 ± 0.24	1.96 ± 0.13	2.28 ± 0.18	I-IV
Adaptation	0.12 ± 0.01	0.02 ± 0.03	0.06 ± 0.01	0.03 ± 0.01	0.03 ± 0.004	I-II, I-III, I-IV, I–V, III-IV, III-V
Repolarization speed (mV/ms)	18.17 ± 2.95	47.29 ± 0.1	17.66 ± 2.62	25.37 ± 1.65	23.56 ± 1.69	I-II, II-III, II-IV, II-V
Input resistance (GΩ)	1.30 ± 0.31	0.23 ± 0.08	0.79 ± 0.38	1.26 ± 0.17	0.92 ± 0.14	
Accommodation (mV)	19.67 ± 2.95	2.07 ± 0.73	6.79 ± 3.38	32.15 ± 2.17	5.16 ± 0.57	I-II, I-III, I-IV, I–V, II-IV, III-IV, IV-V

Table 1 outlines the six AP characteristics and their values utilized to categorize the firing patterns from patched hESC-derived neurons into five types (Types I–V). AP = Action potential.

at 6-weeks, SE mice with transplanted cells showed significantly shorter latencies to first platform crossing (Student's *t*-test, *p < .05, **p < .03; Fig. 5C), and an increased number of platform crossings (Student's *t*-test, *p < .05; Fig. 5D), consistent with improved hippocampal-dependent spatial learning. Additionally, mice with transplants spent significantly more time in the target quadrant compared to the opposite and adjacent quadrants during the probe trial, when compared to media controls that did not show a preference for quadrant location (ANOVA ***p < .01, *P < .05) (Fig. 5E, S6E). Naive controls swam a total of 18.487 ± 0.3185 meters (m) at a swim speed of 0.308 ± 0.0053 m/s(s), SE mice with media injections swam 17.802 ± 0.6565 m at a swim speed of 0.2967 ± 0.0109 m/s, and SE mice with transplanted cells swam 18.367 ± 0.3932 m at a swim speed of 0.3061 ± 0.0066 m/s (Swim Path Length $p = .5493$, ANOVA; Swim Speed $p = .5453$, ANOVA). Swim distance and speed for all three treatment groups were comparable, suggesting that increased dwell times in the platform quadrant were the result of improved cognitive memory in SE mice with transplants. Mice were retested at 10 weeks and memory improvements in SE mice with transplants were maintained during the training phase (two-way Repeated Measures ANOVA, p < .05; Fig. S6A). Additionally, at 10 weeks, transplant mice continued to show significantly lower latencies to first platform crossing during the probe trial (Student's *t*-test, **p < .03, ***p < .01; Fig. S6C), and spent significantly more time in the target quadrant, however they did not show significant improvements in the number of platform crossings (Fig. S6D). Representative ANY-maze swim path plots of animals from the three treatment groups at the beginning (Day 1) and end (Day 5) of training and during the probe trial suggest that SE mice with transplants showed improved search strategies compared to media controls at both time points (Fig. 5B; S6B). Overall, these data show that SE mice with transplants exhibited improved hippocampal-dependent spatial memory at six and ten weeks.

3.6. SE mice with hippocampal transplants of hESNPs did not show reductions in seizure frequency, duration, or severity compared with SE mice without transplants

To determine whether transplanted hESNPs suppressed seizures in SE mice, we conducted continuous V-EEG recordings comparing SE mice with control media injections to SE mice that received hippocampal hESNP transplants. EEG traces show interictal and seizure activity in an SE mouse with a control media injection and an SE mouse with transplant (Fig. 6A). Both the media injected control and the SE mouse with a transplant displayed similar electrographic activity during seizures. To determine whether mice with hESNP transplants showed similar patterns of seizures compared to the controls, we plotted seizures per day for 39 mice (21 SE mice with media injections; 18 SE mice with hESNP transplants, including 3 mice that developed neural tumor-like NSC clusters). All of the mice had confirmed spontaneous recurrent seizures and at least eleven days of continuous V-EEG recording (the mean recording interval for all of the mice was 31 days; in the control SE mice, the mean interval of recording was 29 days (SD ± 6.4), the minimum was 19 days and the maximum was 40 days. For the SE mice with hESNP transplants, the mean interval of recording was 32 days (SD ± 6.5), the minimum was 11 days, and the maximum was 40 days. An additional 7 SE mice were excluded from EEG analyses due to insufficient recording intervals of < 11 days.

The SE mice exhibited variable numbers of seizures within and between groups, and Fig. 6B shows this range in 10 representative mice (5 media injected and 5 mice with transplants). SE mice from both the control and experimental groups displayed clustered patterns of spontaneous recurrent seizures, with comparable variation between groups. To test whether the transplants reduced the incidence of seizures, we compared the average number of seizures/day for the entire interval of EEG recording in control SE mice to SE mice with hESNP transplants. Comparing treatment groups, we found no significant differences in the average number of seizures/day ($p = .17$, negative binomial, Fig. 6C). The 3 SE mice with transplant-derived tumor-like NSC clusters (Fig. 6C, unfilled triangles), displayed similar numbers of seizures per day, suggesting cell clustering in these mice did not appear to alter the incidence of seizures. To determine whether the mice with hESNP transplants showed reduced seizure severity, we analyzed the average duration of seizures between groups. The results showed no significant effects of transplants on seizure duration ($p = .67$, Student's *t*-test, Fig. 6D). Furthermore, behavioral scoring of seizure severity using the modified Racine scale showed no significant differences between the treatment groups ($p = .24$, mixed model, Fig. 6E). Mice with similar-sized transplants ($n = 3$) containing cells with comparable hESNP differentiation displayed substantial variations in both the total number of seizures and the average number of seizures per day. Overall, our data indicate that the hESNP transplants in SE mice did not reduce seizures. Given that our grafts contained considerable numbers of immature neural progenitors and more mature neuronal types, these findings suggest that despite the presence of functionally mature neurons, the differentiated neurons were not sufficiently functionally integrated into the hippocampus to provide levels of inhibition required to suppress limbic seizures.

4. Discussion

Given the interest in cell replacement therapies for the treatment of epilepsy, we explored whether an hESC source could produce the appropriate functioning interneuron subtypes and alter the seizure profile and behavior in a mouse model. We examined the fate of ventralized hESNPs following *in vitro* culture with mouse cortical astrocytes, or transplantation to the hippocampus of naïve and pilocarpine-treated mice that developed spontaneous recurrent limbic seizures. Our *in vitro* analyses showed significant neural maturation over time, with increased neuronal marker expression. In accordance with published reports (Nicholas et al., 2013), maturation of hESNPs required long-term co-culture with mouse cortical astrocytes. We observed expression of both MGE-like and CGE-like interneuron markers, consistent with our previous transcriptome analyses showing higher levels of the CGE marker COUP-*TfI*I in the NKX2.1:GFP negative cell population (Chen et al., 2016).

Transplanted cells required 16–24 weeks to yield 70–85% Hu- and

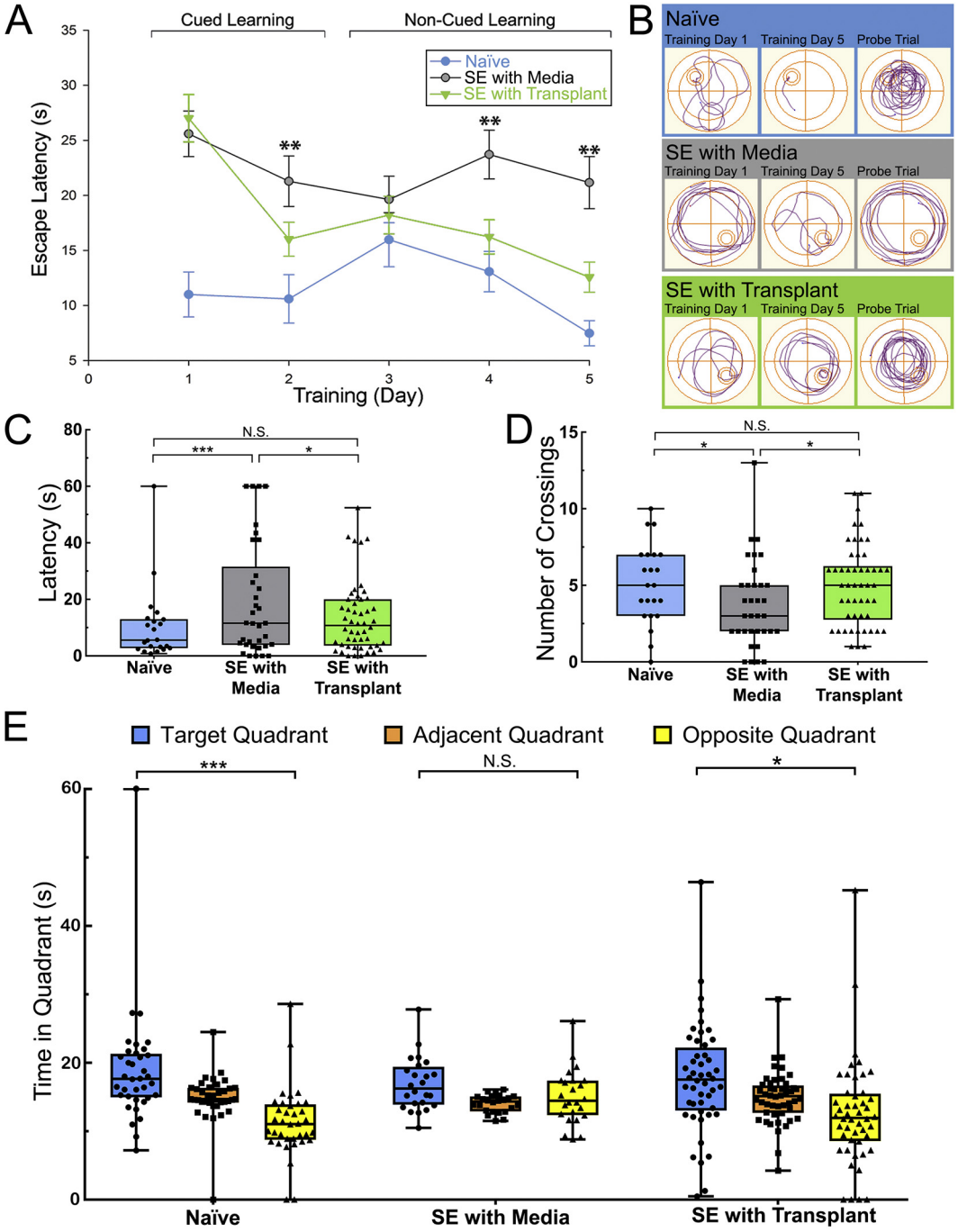

Fig. 5. SE mice with hESNP transplants showed significant improvements in cognition at 6 and 10 weeks post-transplantation. See also fig. S6.
A) Escape latencies to platform during training in the Morris water maze for naïve mice, SE mice with media injection and SE mice with hESNP transplants ($p < .05$, two-way Repeated Measures Anova) at 6 weeks. B) Representative ANY-maze swim path plots of individual animals from the three treatment groups at the start (Day 1) and end (Day 5) of training and the probe trial. C) Latencies to first platform crossing during the day 6 probe trial (Student's *t*-test, *p < .05, **p < .03). D) Probe trial platform crossing for the 3 groups (Student's *t*-test, *p < .05). E) Probe trial quadrant dwell times for the 3 groups (ANOVA, *p < .05, ***p < .01). Naïve $n = 11$, SE with media $n = 17$, SE mice with hESNP transplants $n = 25$.

NeuN- positive neurons that matured into subtypes of GABAergic interneurons after transplantation into either naive or SE mice. We identified cells with immature APs, although a majority of the cells displayed mature firing patterns. Despite maturation of many of the transplanted cells, a proliferative hESNP population remained well beyond 16 weeks, and was likely the source of tumor-like NSC clusters observed. The extent of neural NSC cluster formation varied for different rounds of cell transplantation, even though all transplants were performed using ventralized ESNPs differentiated, characterized, frozen, and stored in aliquots to ensure standardization of transplant batches. To avoid transplantation of proliferative ESNPs, various studies used the Notch inhibitor DAPT to promote terminal differentiation and FACS-mediated isolation to enrich for a more mature cell population (Nicholas et al., 2013; Cunningham et al., 2014). In our hands, both approaches significantly reduced cell viability, with up to a 30% reduction in cell survival immediately following FACS-isolation, and < 3% of FACS-isolated cells survived up to 6 weeks post-transplantation. Identification of an interneuron progenitor-specific cell-

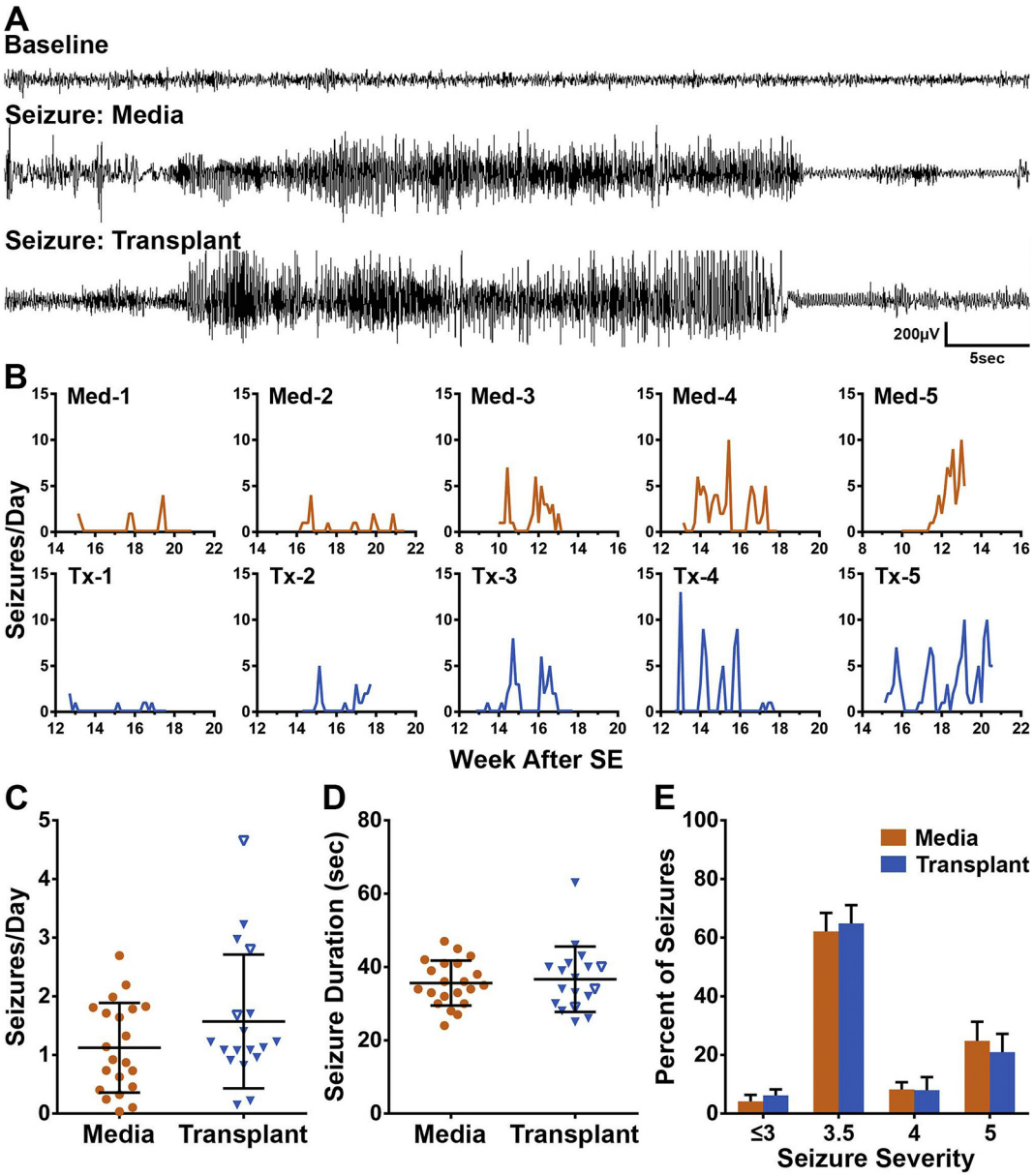

Fig. 6. SE mice with hippocampal transplants of hESNPs were comparable to control SE mice without transplants in terms of seizure frequency, duration, and severity.

A) Representative EEG traces from SE mice that received either media or transplants of hESNPs. The baseline trace is from the media injected mouse. B) Summary plots showing seizure frequency *vs.* day for 10 representative mice. Each graph depicts an individual mouse and the mildest cases are shown on the left; more severe cases to the right. C) Scatterplot shows average seizures/day for each experimental animal. No significant differences were found between groups in seizures per day (p = .17, negative binomial). D) Scatter plots of seizure duration. No significant differences were found between groups (p = .67, Student's t-test). Middle bars indicate the group means; upper and lower bars = S.E.M. Filled triangles represent mice with transplants. Unfilled triangles represent mice with transplant-derived tumor-like NSC clusters (n = 3). E) Graph showing behavioral scoring of seizure severity based on a modified Racine scale. No significant differences were found between the treatment groups (p = .41, mixed model). Error bars = S.E.M. Control group receiving media injections, n = 21 mice; experimental group receiving human NSCs, n = 18 mice.

surface marker could facilitate isolation of a non-genetically modified, more mature population of MGE-like cells.

Our findings that hESNPs cells differentiated into mature interneurons after transplantation led us to test whether these grafts promoted functional recovery of spatial learning and memory in SE mice. Cunningham and collegues previously showed that PSC-derived cell transplants significantly improved cognitive performance in the Y-maze, a short-term working memory task. Additonally, mice with transplants spent significantly more time exploring novel objects and exhibited decreased aggression (Cunningham et al., 2014). However, they did not assess spatial memory changes in mice with transplants. The hippocampus plays a major role in both spatial and episodic learning and memory (Martin and Clark, 2007; Neves et al., 2008; Squire, 2004) and when lesioned, rodents display decreased ability to navigate their spatial environment in the Morris water maze (Liu et al., 1994; Martin and Clark, 2007; Titiz et al., 2014). Using the Morris water maze test, we observed significant improvements in hippocampal-dependent spatial memory in SE mice that had transplants, when compared to SE mice with media injections, and these effects were evident as early as 6 weeks after transplantation, well before the time when the majority of transplanted cells reached maturity. Our data suggest that significant cognitive improvement in the Morris water

maze task may be due to a minority of mature transplant-derived neurons integrating into the hippocampus. These cells may act synaptically, or through ambient release of GABA to promote hippocampal-dependent learning and memory. Alternatively, the hESNPs may act through a trophic effect, either by releasing factors that enhance learning and memory, or by reducing inflamation which impairs learning.

Despite improved spatial learning and memory, the SE mice with transplanted cells did not show significant seizure suppression. Previous studies reported seizure suppression and increased inhibitory post-synaptic currents in excitatory cells in the vicinity of transplanted interneurons, following transplantation of fetal mouse MGE-derived interneurons (Henderson et al., 2014; Hunt et al., 2013). Our EEG analyses did not show any significant effects of the transplanted cells on seizure frequency, duration, or severity in SE mice. The presence of tumor-like NSC clusters does not explain the absence of seizure suppression, given our observation that mice with no visible tumor-like NSC clusters did not display transplant-mediated seizure suppression compared to media-injected controls. Cunningham and colleagues reported reduced seizure frequencies in SE mice with hESNP-derived interneuron transplants compared to SE media-injected control mice (Cunningham et al., 2014). Discrepancies between our studies and their work might be attributed to the greater heterogeneity of the cell population that we transplanted. Cunningham et al. successfully implemented a FACS-based enrichment step, yielding more mature cells for transplantation. Of note, pilocarpine treatment leads to clusters of seizures that can only be observed over weeks of EEG recording (Mazzuferi et al., 2012). We analyzed on average, about 32 days of continuous EEG recordings for each SE mouse, as early as 10.8 weeks and as late as 20.8 weeks after transplantation, in contrast to 5–10 days of EEG recordings per mouse starting 3 months after transplantation by Cunningham et al.. Our extended EEG studies are more likely to detect spontaneous seizures but may miss short-term windows of transplant-mediated seizure suppression, as observed by Cunningham et al., 2014. Alternatively, the hESNP-derived GABAergic interneurons in our study may not have formed synaptic connections with host neurons involved in seizure propogation. Future studies examining the maturation of synaptic connections between transplanted and endogenous neurons could address this question through use of trans-synaptic tracing methods (Falkner et al., 2016; Grealish et al., 2015). Furthermore, future investigators may test functional integration into host brain circuits by directly activating transplanted cells using optogenetic stimulation while recording from endogenous excitatory cells (Cunningham et al., 2014; Henderson et al., 2014; Nicholas et al., 2013; Steinbeck et al., 2015).

Funding

This work was funded by the Connecticut Regenerative Medicine Research Fund to L.G, J.R.N, and G.A. [grant 13-SCC-WES-01].

Author contributions

N.C.A., hESNP *in vitro* and *in vivo* differentiation and characterization. C.Y.C., C.D., T.B., long-term hESNP-astrocyte co-culture and analysis. N.C.A, F.A.H., hESNP stereotactic injections. M.V.Z. conducted behavior analyses. S.S., J.G., patch clamp analyis, N.C.A., staining, imaging and reconstruction of biocytin-filled cells. M.V.Z., D.B.L., F.A.H., N.C.A., S.S., C.Y.C., SE induction, electrode implantation surgery, video monitoring and EEG data collection. N.C.A., D.B.L., EEG data analysis. N.C.A., M.V.Z., S.S., D.B.L., figures and legends. N.C.A., L.G., manuscript writing. L.G., G.A., J.R.N., project design, conceptualization, funding acquisition, project supervision, data analysis, manuscript edits and final approval. All authors reviewed, edited and approved the manuscript.

The authors report no conflicts of interest.

Acknowledgements

We wish to thank Dr. Stewart A. Anderson and Dr. Andrew Elefanty for the HES3 NKX2.1:GFP hESCs. We would also like to thank Dr. Valerie Nazzaro at Wesleyan's quantitative analysis center for assistance with data and statistical analyses, Dr. Chelsea Lassiter, and Katherine W. Henderson for technical assistance with initial pilot experiments, Toria Bobbitt for assistance with LOREX, Kevin Cobbol for data entry, and Sandy Becker for careful reading of, and providing comments on the manuscript.

Appendix A. Supplementary data

Supplementary data to this article can be found online at https://doi.org/10.1016/j.scr.2018.10.007.

References

Anderson, S.A., Marin, O., Horn, C., Jennings, K., Rubenstein, J.L., 2001. Distinct cortical migrations from the medial and lateral ganglionic eminences. Development 128, 353–363.
Baraban, S.C., Southwell, D.G., Estrada, R.C., Jones, D.L., Sebe, J.Y., Alfaro-Cervello, C., Garcia-Verdugo, J.M., Rubenstein, J.L., Alvarez-Buylla, A., 2009. Reduction of seizures by transplantation of cortical GABAergic interneuron precursors into Kv1.1 mutant mice. Proc. Natl. Acad. Sci. U. S. A. 106, 15472–15477.
Cascino, G.D., Jack Jr., C.R., Parisi, J.E., Marsh, W.R., Kelly, P.J., Sharbrough, F.W., Hirschorn, K.A., Trenerry, M.R., 1992. MRI in the presurgical evaluation of patients with frontal lobe epilepsy and children with temporal lobe epilepsy: pathologic correlation and prognostic importance. Epilepsy Res. 11, 51–59.
Chen, C.Y., Plocik, A., Anderson, N.C., Moakley, D., Boyi, T., Dundes, C., Lassiter, C., Graveley, B.R., Grabel, L., 2016. Transcriptome and in vitro differentiation profile of human embryonic stem cell derived NKX2.1-positive neural progenitors. Stem Cell Rev. 12, 744–756.
Chohan, M.O., Moore, H., 2016. Interneuron progenitor transplantation to treat CNS dysfunction. Front. Neural. Circuits 10, 64.
Cunningham, M., Cho, J.H., Leung, A., Savvidis, G., Ahn, S., Moon, M., Lee, P.K., Han, J.J., Azimi, N., Kim, K.S., et al., 2014. hPSC-derived maturing GABAergic interneurons ameliorate seizures and abnormal behavior in epileptic mice. Cell Stem Cell 15, 559–573.
de Lanerolle, N.C., Kim, J.H., Robbins, R.J., Spencer, D.D., 1989. Hippocampal interneuron loss and plasticity in human temporal lobe epilepsy. Brain Res. 495, 387–395.
de Lanerolle, N.C., Lee, T.S., Spencer, D.D., 2010. Astrocytes and epilepsy. Neurotherapeutics 7, 424–438.
de Lanerolle, N.C., Lee, T.S., Spencer, D.D., 2012. Histopathology of human epilepsy. In: Noebels, J.L., Avoli, M., Rogawski, M.A., Olsen, R.W., Delgado-Escueta, A.V. (Eds.), Jasper's Basic Mechanisms of the Epilepsies. National Center for Biotechnology Information, US.
Etlin, A., Braz, J.M., Kuhn, J.A., Wang, X., Hamel, K.A., Llewellyn-Smith, I.J., Basbaum, A.I., 2016. Functional synaptic integration of forebrain GABAergic precursors into the adult spinal cord. J. Neurosci. 36, 11634–11645.
Falkner, S., Grade, S., Dimou, L., Conzelmann, K.K., Bonhoeffer, T., Gotz, M., Hubener, M., 2016. Transplanted embryonic neurons integrate into adult neocortical circuits. Nature 539, 248–253.
Fandel, Thomas M., Trivedi, A., Nicholas, Cory R., Zhang, H., Chen, J., Martinez, Aida F., Noble-Haeusslein, Linda J., Kriegstein, Arnold R., 2016. Transplanted human stem cell-derived interneuron precursors mitigate mouse bladder dysfunction and central neuropathic pain after spinal cord injury. Cell Stem Cell 19, 544–557.
Flames, N., Pla, R., Gelman, D.M., Rubenstein, J.L., Puelles, L., Marin, O., 2007. Delineation of multiple subpallial progenitor domains by the combinatorial expression of transcriptional codes. J. Neurosci. 27, 9682–9695.
Gelman, D.M., Marin, O., 2010. Generation of interneuron diversity in the mouse cerebral cortex. Eur. J. Neurosci. 31, 2136–2141.
Germain, N.D., Banda, E.C., Becker, S., Naegele, J.R., Grabel, L.B., 2013. Derivation and isolation of NKX2.1-positive basal forebrain progenitors from human embryonic stem cells. Stem Cells Dev. 22, 1477–1489.
Goulburn, A.L., Stanley, E.G., Elefanty, A.G., Anderson, S.A., 2012. Generating GABAergic cerebral cortical interneurons from mouse and human embryonic stem cells. Stem Cell Res. 8, 416–426.
Grealish, S., Heuer, A., Cardoso, T., Kirkeby, A., Jönsson, M., Johansson, J., Björklund, A., Jakobsson, J., Parmar, M., 2015. Monosynaptic tracing using modified rabies virus reveals early and extensive circuit integration of human embryonic stem cell-derived neurons. Stem Cell Rep. 4, 975–983.
Hammad, M., Schmidt, S.L., Zhang, X., Bray, R., Frohlich, F., Ghashghaei, H.T., 2015. Transplantation of GABAergic interneurons into the neonatal primary visual cortex reduces absence seizures in stargazer mice. Cereb. Cortex 25, 2970–2979.
Hansen, D.V., Lui, J.H., Flandin, P., Yoshikawa, K., Rubenstein, J.L., Alvarez-Buylla, A., Kriegstein, A.R., 2013. Non-epithelial stem cells and cortical interneuron production in the human ganglionic eminences. Nat. Neurosci. 16, 1576–1587.
Henderson, K.W., Gupta, J., Tagliatela, S., Litvina, E., Zheng, X., Van Zandt, M.A., Woods, N., Grund, E., Lin, D., Royston, S., et al., 2014. Long-term seizure suppression and

optogenetic analyses of synaptic connectivity in epileptic mice with hippocampal grafts of GABAergic interneurons. J. Neurosci. 34, 13492–13504.
Hermann, B.P., Seidenberg, M., Bell, B., 2002. The neurodevelopmental impact of childhood onset temporal lobe epilepsy on brain structure and function and the risk of progressive cognitive effects, Prog. Brain Res. Elsevier, pp. 429–438.
Hunt, R.F., Girskis, K.M., Rubenstein, J.L., Alvarez-Buylla, A., Baraban, S.C., 2013. GABA progenitors grafted into the adult epileptic brain control seizures and abnormal behavior. Nat. Neurosci. 16, 692–697.
Jokeit, H., Ebner, A., 1999. Long term effects of refractory temporal lobe epilepsy on cognitive abilities: a cross sectional study. J. Neurol. Neurosurg. Psychiatry 67, 44–50.
Kepecs, A., Fishell, G., 2014. Interneuron cell types are fit to function. Nature 505, 318–326.
Kim, T.G., Yao, R., Monnell, T., Cho, J.H., Vasudevan, A., Koh, A., Peeyush, K.T., Moon, M., Datta, D., Bolshakov, V.Y., et al., 2014. Efficient specification of interneurons from human pluripotent stem cells by dorsoventral and rostrocaudal modulation. Stem Cells 32, 1789–1804.
Lancaster, M.A., Renner, M., Martin, C.A., Wenzel, D., Bicknell, L.S., Hurles, M.E., Homfray, T., Penninger, J.M., Jackson, A.P., Knoblich, J.A., 2013. Cerebral organoids model human brain development and microcephaly. Nature 501, 373–379.
Li, X.J., Zhang, X., Johnson, M.A., Wang, Z.B., Lavaute, T., Zhang, S.C., 2009. Coordination of sonic hedgehog and Wnt signaling determines ventral and dorsal telencephalic neuron types from human embryonic stem cells. Development 136, 4055–4063.
Liu, Z., Gatt, A., Werner, S.J., Mikati, M.A., Holmes, G.L., 1994. Long-term behavioral deficits following pilocarpine seizures in immature rats. Epilepsy Res. 19, 191–204.
Liu, Y., Liu, H., Sauvey, C., Yao, L., Zarnowska, E.D., Zhang, S.C., 2013a. Directed differentiation of forebrain GABA interneurons from human pluripotent stem cells. Nat. Protoc. 8, 1670–1679.
Liu, Y., Weick, J.P., Liu, H., Krencik, R., Zhang, X., Ma, L., Zhou, G.M., Ayala, M., Zhang, S.C., 2013b. Medial ganglionic eminence-like cells derived from human embryonic stem cells correct learning and memory deficits. Nat. Biotechnol. 31, 440–447.
Loscher, W., Ebert, U., Lehmann, H., Rosenthal, C., Nikkhah, G., 1998. Seizure suppression in kindling epilepsy by grafts of fetal GABAergic neurons in rat substantia nigra. J. Neurosci. Res. 51, 196–209.
Ma, T., Wang, C., Wang, L., Zhou, X., Tian, M., Zhang, Q., Zhang, Y., Li, J., Liu, Z., Cai, Y., et al., 2013. Subcortical origins of human and monkey neocortical interneurons. Nat. Neurosci. 16, 1588–1597.
Machold, R., Hayashi, S., Rutlin, M., Muzumdar, M.D., Nery, S., Corbin, J.G., Gritli-Linde, A., Dellovade, T., Porter, J.A., Rubin, L.L., et al., 2003. Sonic hedgehog is required for progenitor cell maintenance in telencephalic stem cell niches. Neuron 39, 937–950.
Maisano, X., Litvina, E., Tagliatela, S., Aaron, G.B., Grabel, L.B., Naegele, J.R., 2012. Differentiation and functional incorporation of embryonic stem cell-derived GABAergic interneurons in the dentate gyrus of mice with temporal lobe epilepsy. J. Neurosci. 32, 46–61.
Maroof, A.M., Keros, S., Tyson, J.A., Ying, S.W., Ganat, Y.M., Merkle, F.T., Liu, B., Goulburn, A., Stanley, E.G., Elefanty, A.G., et al., 2013. Directed differentiation and functional maturation of cortical interneurons from human embryonic stem cells. Cell Stem Cell 12, 559–572.
Martin, S.J., Clark, R.E., 2007. The rodent hippocampus and spatial memory: from synapses to systems. Cell. Mol. Life Sci. 64, 401–431.
Mazzuferi, M., Kumar, G., Rospo, C., Kaminski, R.M., 2012. Rapid epileptogenesis in the mouse pilocarpine model: video-EEG, pharmacokinetic and histopathological characterization. Exp. Neurol. 238, 156–167.
Muller, C.J., Groticke, I., Bankstahl, M., Loscher, W., 2009. Behavioral and cognitive alterations, spontaneous seizures, and neuropathology developing after a pilocarpine-induced status epilepticus in C57BL/6 mice. Exp. Neurol. 219, 284–297.
Neves, G., Cooke, S.F., Bliss, T.V., 2008. Synaptic plasticity, memory and the hippocampus: a neural network approach to causality. Nat. Rev. Neurosci. 9, 65–75.
Nicholas, C.R., Chen, J., Tang, Y., Southwell, D.G., Chalmers, N., Vogt, D., Arnold, C.M., Chen, Y.J., Stanley, E.G., Elefanty, A.G., et al., 2013. Functional maturation of hPSC-derived forebrain interneurons requires an extended timeline and mimics human neural development. Cell Stem Cell 12, 573–586.
Parent, J.M., Murphy, G.G., 2013. Ganglionic eminence graft pre-eminence in epilepsy. Nat. Neurosci. 16, 656–658.
Shetty, A.K., Bates, A., 2016. Potential of GABA-ergic cell therapy for schizophrenia, neuropathic pain, and Alzheimers and Parkinsons diseases. Brain Res. 1638, 74–87.
Shetty, A.K., Hattiangady, B., 2007. Concise review: prospects of stem cell therapy for temporal lobe epilepsy. Stem Cells 25, 2396–2407.
Squire, L.R., 2004. Memory systems of the brain: a brief history and current perspective. Neurobiol. Learn. Mem. 82, 171–177.
Steinbeck, J.A., Choi, S.J., Mrejeru, A., Ganat, Y., Deisseroth, K., Sulzer, D., Mosharov, E.V., Studer, L., 2015. Optogenetics enables functional analysis of human embryonic stem cell-derived grafts in a Parkinson's disease model. Nat. Biotechnol. 33, 204–209.
Sussel, L., Marin, O., Kimura, S., Rubenstein, J.L., 1999. Loss of Nkx2.1 homeobox gene function results in a ventral to dorsal molecular respecification within the basal telencephalon: evidence for a transformation of the pallidum into the striatum. Development 126, 3359–3370.
Titiz, A.S., Mahoney, J.M., Testorf, M.E., Holmes, G.L., Scott, R.C., 2014. Cognitive impairment in temporal lobe epilepsy: role of online and offline processing of single cell information. Hippocampus 24, 1129–1145.
Tyson, J.A., Goldberg, E.M., Maroof, A.M., Xu, Q., Petros, T.J., Anderson, S.A., 2015. Duration of culture and sonic hedgehog signaling differentially specify PV versus SST cortical interneuron fates from embryonic stem cells. Development 142, 1267–1278.
Waldau, B., Hattiangady, B., Kuruba, R., Shetty, A.K., 2010. Medial ganglionic eminence-derived neural stem cell grafts ease spontaneous seizures and restore GDNF expression in a rat model of chronic temporal lobe epilepsy. Stem Cells 28, 1153–1164.
Wolf, H.K., Campos, M.G., Zentner, J., Hufnagel, A., Schramm, J., Elger, C.E., Wiestler, O.D., 1993. Surgical pathology of temporal lobe epilepsy. Experience with 216 cases. J. Neuropathol. Exp. Neurol. 52, 499–506.
Xu, Q., Wonders, C.P., Anderson, S.A., 2005. Sonic hedgehog maintains the identity of cortical interneuron progenitors in the ventral telencephalon. Development 132, 4987–4998.
Zipancic, I., Calcagnotto, M.E., Piquer-Gil, M., Mello, L.E., Alvarez-Dolado, M., 2010. Transplant of GABAergic precursors restores hippocampal inhibitory function in a mouse model of seizure susceptibility. Cell Transplant. 19, 549–564.